

# Parallel Multi-Stage Preconditioners with Adaptive Setup for the Black Oil Model\*

Li Zhao<sup>†</sup>, Chunsheng Feng<sup>†</sup>, Chensong Zhang<sup>‡</sup>, and Shi Shu<sup>†</sup>

**Abstract.** The black oil model is widely used to describe multiphase porous media flow in the petroleum industry. The fully implicit method features strong stability and weak constraints on time step-sizes; hence, commonly used in the current mainstream commercial reservoir simulators. In this paper, a CPR-type preconditioner with an adaptive “setup phase” is developed to improve parallel efficiency of petroleum reservoir simulation. Furthermore, we propose a multi-color Gauss-Seidel (GS) algorithm for algebraic multigrid method based on the coefficient matrix of strong connections. Numerical experiments show that the proposed preconditioner can improve the parallel performance for both OpenMP and CUDA implements. Moreover, the proposed algorithm yields good parallel speedup as well as same convergence behavior as the corresponding single-threaded algorithm. In particular, for a three-phase benchmark problem, the parallel speedup of the OpenMP version is over 6.5 with 16 threads and the CUDA version reaches more than 9.5.

**Key words.** Black oil model; fully implicit method; parallel computing; multi-color Gauss-Seidel smoother; multi-stage preconditioners.

**AMS subject classifications.** 49M20, 65F10, 68W10, 76S05

**1. Introduction.** Research on petroleum reservoir simulation can be traced back to the 1950s. To describe and predict the transportation of hydrocarbons, various mathematical models have been established, such as the black oil model, compositional model, thermal recovery model, and chemical flooding model, etc [1–3]. The black oil model consists of multiple coupled nonlinear partial differential equations (PDEs). It is a fundamental mathematical model to describe the three-phase flow in petroleum reservoirs and is widely used in simulating primary and secondary recovery.

After 70 years of development, there is a large amount of research work on the numerical methods of the black oil model; for instance, Simultaneous Solution (SS) method [4], Fully Implicit Method (FIM) [5], IMPLICIT Pressure Explicit Saturation (IMPES) method [6], and Adaptive Implicit Method (AIM) [7]. Compared with other methods, FIM is commonly-used in the mainstream commercial reservoir simulators [8–10] because of its unconditional stability nature with respect to time step-sizes. However, a coupled Jacobian linear algebraic system needs to be solved in each Newton iteration step. Due to the complexity of the practical engineering problem, such systems are difficult to solve with traditional linear solvers. In the reservoir simulation, the solution time of Jacobian systems easily occupies more than 80% of the whole simulation time. Therefore, how to efficiently solve the coupled Jacobian systems, especially on modern computers, is a problem that still attracts a lot attentions nowadays.

Typically, linear solution methods can be divided into two phases, the “setup phase” (SETUP) and the “solve phase” (SOLVE). These methods can usually be categorized as the direct methods [11] and the iterative methods [12]. Compared with the direct methods, the iterative methods have the advantages of low memory/computation complexity and potentially good parallel scalability [13]. The linear algebraic systems arising from fully implicit petroleum reservoir simulation are usually solved by iterative methods. In particular, the Krylov subspace methods [12] (such as GMRES and BiCGstab) are frequently adopted. For linear systems with poor condition, the preconditioning technique [14, 15] is needed to accelerate the convergence

---

\*Manuscript Version 1, [January 7, 2022](#).

<sup>†</sup>School of Mathematics and Computational Science, Xiangtan University, Xiangtan, Hunan 411105, P. R. China.

<sup>‡</sup>Academy of Mathematics and System Sciences, Beijing 100190, P. R. China. (Corresponding author: Chensong Zhang, Email: [zhangcs@lsec.cc.ac.cn](mailto:zhangcs@lsec.cc.ac.cn)).

of the iterative methods. The preconditioners for reservoir simulation include: Incomplete LU (ILU) factorization [16, 17], Algebraic MultiGrid (AMG) [18–25], Constrained Pressure Residual (CPR) [26–29], and Multi-Stage Preconditioner (MSP) [30–32]. The ILU method is relatively easy to implement; but as the problem size increases, its convergence deteriorates. The advantages of the AMG method are easy-to-use and very effective to elliptic problems. Owing to the asymmetry, heterogeneity, and nonlinear coupling feature of the petroleum reservoir problems, the performance of the AMG methods also deteriorates. The CPR method combines the advantages of ILU and AMG; and the MSP method is a generalization of CPR. Thus, the CPR and MSP preconditioners are widely used in petroleum reservoir problems.

As multi-core and many-core architectures become more and more popular, parallel computing for petroleum reservoir simulation is now a subject of great interest. In recent years, there has been some work on parallel algorithms for reservoir problems; see [33–45] and references therein. For example, Feng et al. [35] designed an OpenMP parallel algorithm with high efficiency and low memory cost for standard interpolation and coarse grid operator of AMG, under the framework of Fast Auxiliary Space Preconditioning (FASP) [46]. Wu et al. [36] developed a Method of Subspace Correction (MSC) based on [35] and realized the cost-effective OpenMP parallel reservoir numerical simulation [39]. Sudan et al. [42] designed a GPU parallel algorithm based on the METIS [47] partition for the IMPES method. Yang et al. [44] studied the GPU parallel algorithm of ILU and AMG based on the hybrid sparse storage format, i.e., Hybrid of ELL and CSR (HEC), and so on.

In this paper, we focus on the solution method for the linear algebraic systems arising from the fully implicit discretization of the black oil model, aiming at improving the parallel efficiency of the CPR preconditioner. The main contributions of this work are listed as follows:

- We propose an adaptive SETUP CPR preconditioner (denoted as ASCPR) to improve the efficiency and parallel performance of the solver. A practical adaptive criterion is proposed to judge whether a new SETUP is necessary. The technology can bring two benefits: (1) The efficiency of the solver is improved because the number of SETUP calls can be significantly reduced; (2) The parallel performance is improved because there are many essentially sequential algorithms in the SETUP (the parallel speedup of these algorithms is low).
- We propose an efficient parallel algorithm for the Gauss-Seidel (GS) relaxation in AMG methods. Starting from the strong connections of coefficient matrix, we design an algorithm for algebraic multi-color grouping. The algorithm has two desirable features: (1) Not relying on the grid (completely transformed into algebraic behavior); (2) Yielding same convergence behavior as the corresponding single-threaded algorithm. Furthermore, we introduce an adjustable strength threshold to filter small matrix entries (enhancing the sparseness) to improve the parallel performance of the algorithm.

The rest of the paper is organized as follows. Section 2 introduces the black oil model and its fully implicit discrete systems. Section 3 reviews the CPR-type preconditioners. In Section 4, an adaptive SETUP CPR preconditioner is proposed. In Section 5, the parallel implementation of multi-color GS based on the coefficient matrix of strong connections is given. In Section 6, numerical experiments are given. Section 7 summarizes the work of this paper.

## 2. Preliminaries.

**2.1. The black oil model.** This paper considers the following three-phase standard black oil model of water, oil, or gas in porous media [1–3]. The mass conservation equations of water, oil, and gas, respectively, are

$$(2.1) \quad \frac{\partial}{\partial t} \left( \phi \frac{S_w}{B_w} \right) = -\nabla \cdot \left( \frac{1}{B_w} \mathbf{u}_w \right) + \frac{Q_w}{B_w},$$

$$(2.2) \quad \frac{\partial}{\partial t} \left( \phi \frac{S_o}{B_o} \right) = -\nabla \cdot \left( \frac{1}{B_o} \mathbf{u}_o \right) + \frac{Q_O}{B_o},$$

$$(2.3) \quad \frac{\partial}{\partial t} \left[ \phi \left( \frac{S_g}{B_g} + \frac{R_{so} S_o}{B_o} \right) \right] = -\nabla \cdot \left( \frac{1}{B_g} \mathbf{u}_g + \frac{R_{so}}{B_o} \mathbf{u}_o \right) + \frac{Q_G}{B_g} + \frac{R_{so} Q_O}{B_o}.$$

Here  $S_\alpha$  is the saturation of phase  $\alpha$  ( $\alpha = w, o, g$  represents the water phase, oil phase, and gas phase, respectively),  $B_\alpha$  is the volume coefficient of phase  $\alpha$ ,  $\mathbf{u}_\alpha$  is the velocity of phase  $\alpha$ ,  $\phi$  is the porosity of the rock,  $R_{so}$  is the dissolved gas-oil ratio, and  $Q_\beta$  is the injection and production rate of component  $\beta$  ( $\beta = W, O, G$  represents the water component, oil component, and gas component, respectively) under the ground standard status.

Assuming that the three-phase fluid flow in porous media satisfies the Darcy's law:

$$(2.4) \quad \mathbf{u}_\alpha = -\frac{\kappa \kappa_{r\alpha}}{\mu_\alpha} (\nabla P_\alpha - \rho_\alpha \mathbf{g} \nabla z), \quad \alpha = w, o, g.$$

where  $\kappa$  is the absolute permeability,  $\kappa_{r\alpha}$  is the relative permeability of phase  $\alpha$ ,  $\mu_\alpha$  is the viscosity coefficient of phase  $\alpha$ ,  $P_\alpha$  is the pressure of phase  $\alpha$ ,  $\rho_\alpha$  is the density of phase  $\alpha$ ,  $\mathbf{g}$  is the gravity acceleration, and  $z$  is the depth.

The unknown quantities  $S_\alpha$  and  $P_\alpha$  in the equations (2.1)-(2.4) also satisfy the following constitutive relation:

- Saturation constraint equation:

$$(2.5) \quad S_w + S_o + S_g = 1.$$

- Capillary pressure equations:

$$(2.6) \quad \begin{aligned} P_w &= P_o - P_{cow}, \\ P_g &= P_o - P_{cgo}, \end{aligned}$$

where  $P_{cow}$  is capillary pressure between the oil and water phases and  $P_{cgo}$  is capillary pressure between the gas and oil phases.

**2.2. Discretization and algorithm flowchart.** The FIM scheme is currently commonly used in the mainstream commercial reservoir simulators. This is the fact that the scheme has the characteristics of strong stability and weak constraint on the time step-sizes. Especially when the nonlinearity of the models is relatively strong, these characteristics highlight the advantages of the FIM.

In this paper, we use FIM to discretize the governing equations (2.1)-(2.3). That is, the time direction is discretized by the backward Euler method and the spatial direction is discretized by the upstream weighted central finite difference method (see [3, 5] for more details). After discretization, the coupled nonlinear algebraic equations are obtained. Such equations are linearized by adopting the Newton method to form the Jacobian system  $Ax = b$  of the reservoir equation with implicit wells, namely:

$$(2.7) \quad \begin{pmatrix} A_{RR} & A_{RW} \\ A_{WR} & A_{WW} \end{pmatrix} \begin{pmatrix} x_R \\ x_W \end{pmatrix} = \begin{pmatrix} b_R \\ b_W \end{pmatrix},$$

where  $A_{RR}$  and  $A_{RW}$  are the derivatives of the reservoir equations for reservoir variables and well variables respectively,  $A_{WR}$  and  $A_{WW}$  are the derivatives of the well equations for reservoir variables and well variables respectively,  $x_R$  and  $x_W$  are reservoir and bottom-hole flowing pressure variables respectively, and  $b_R$  and  $b_W$  are the right-hand side vectors that

correspond to the reservoir fields and the implicit wells, respectively.

The subsystem corresponding to the reservoir equations in the discrete system (2.7) is  $A_{RR}x_R = b_R$ , i.e.,

$$(2.8) \quad \begin{pmatrix} A_{PP} & A_{PS_w} & A_{PS_o} \\ A_{S_w P} & A_{S_w S_w} & A_{S_w S_o} \\ A_{S_o P} & A_{S_o S_w} & A_{S_o S_o} \end{pmatrix} \begin{pmatrix} x_P \\ x_{S_w} \\ x_{S_o} \end{pmatrix} = \begin{pmatrix} b_P \\ b_{S_w} \\ b_{S_o} \end{pmatrix},$$

where  $P, S_w$  and  $S_o$  are primary variables corresponding to oil pressure, water saturation and oil saturation, respectively.

**Remark 1.** For convenience, we do not describe how to deal with well equations in detail.

In the following, we present a general algorithm flowchart of the petroleum reservoir simulation; see Fig. 1.

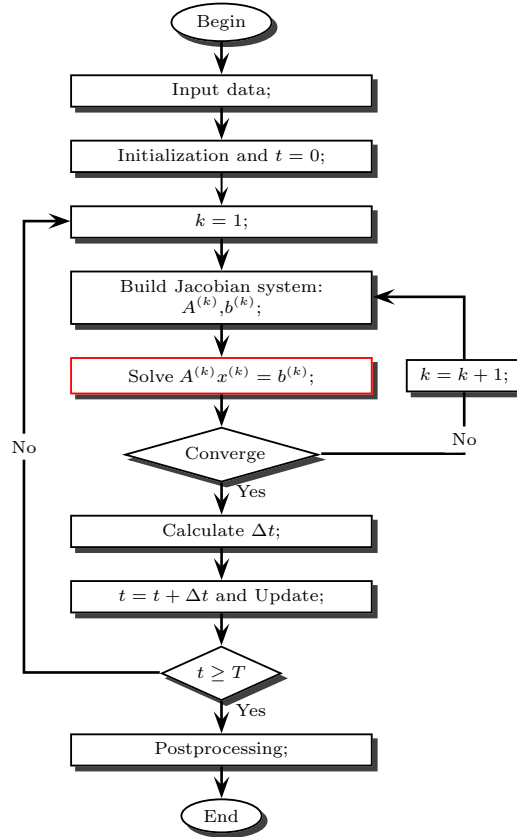


**Fig. 1.** Algorithm flowchart of the petroleum reservoir simulation.

According to Fig. 1, the algorithm flowchart includes two loops: the outer loop (time marching) and the inner loop (Newton iterations). In each Newton iteration, a Jacobian system  $A^{(k)}x^{(k)} = b^{(k)}$  (superscript  $k$  is the number of Newton iterations) needs to be solved, which is the main computational work to be carried out.

**3. The CPR-type preconditioners.** The primary variables usually consists of oil pressure  $P$  and saturations  $S$  (including  $S_w$  and  $S_o$ ) in FIM, which have different mathematical properties, respectively. For example, the pressure equation is parabolic and the saturation equation is hyperbolic [48]. These properties provide a theoretical basis for the design of multiplicative subspace correction methods [14, 15].

**3.1. CPR preconditioner.** First of all, the transfer operator  $\Pi_P : \mathcal{V}_P \rightarrow \mathcal{V}$  is defined, where  $\mathcal{V}_P$  and  $\mathcal{V}$  are the pressure variables space and the variables space of the whole reservoir, respectively. Next, a well-known two-stage preconditioner — the Constrained Pressure Residual (CPR) [26–29] preconditioner  $B$  is defined as:

$$(3.1) \quad I - BA = (I - RA)(I - \Pi_P B_P \Pi_P^T A).$$

where  $B_P$  is solved by the AMG method and the relaxation (or smoothing) operator  $R$  uses the Block ILU (BILU) method [16].

Finally, the CPR preconditioning algorithm is shown in Algorithm 3.1.

---

**Algorithm 3.1** CPR method

---

**Input:**  $A, b, x$ ;

**Output:**  $x$ ;

- 1  $r \leftarrow b - Ax$ ;
  - 2  $x \leftarrow x + \Pi_P B_P \Pi_P^T r$ ;
  - 3  $r \leftarrow b - Ax$ ;
  - 4  $x \leftarrow x + Rr$ .
  - 5 **return**  $x$ .
- 

**3.2. Red-Black GS method.** As we all know, compared with the Jacobi algorithm, the GS algorithm uses the updated values in the iterative process. Hence, the GS algorithm obtains better convergence rate and is widely used as a smoother of AMG. Nowadays, the parallel red-black GS (also referred to multi-color GS) algorithm on structured grid, is pretty mature [12]. We take a 2D structured grid as an example to present two-color and four-color vertex-grouping diagrams; see Fig. 2.

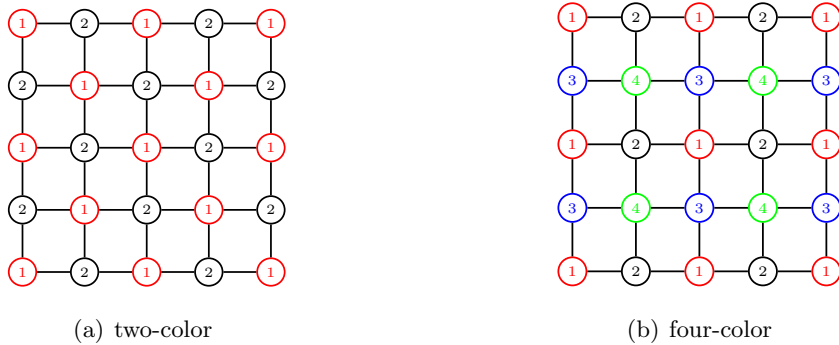


**Fig. 2.** Two-color and four-color vertex-grouping diagrams.

In Fig. 2(a), the vertices are divided into two groups and marked as red and black points, that is, vertex set  $V$  are divided into  $V_1$  and  $V_2$ . In Fig. 2(b), the vertices are divided into four groups and marked as red, black, blue, and green, i.e., vertex set  $V$  are divided into  $V_1, V_2, V_3,$  and  $V_4$ . The multi-color GS algorithm is to perform parallel smoothing on the vertices of the same color, i.e., (1) for the case of two colors, firstly all-red vertices ( $V_1$ ) are smoothed in parallel, then all-black ( $V_2$ ) vertices are smoothed in parallel; (2) for the case of four colors, firstly all-red vertices ( $V_1$ ) are smoothed in parallel, secondly all-black vertices ( $V_2$ ) are smoothed in parallel, thirdly all-blue vertices ( $V_3$ ) are smoothed in parallel, finally all-green vertices ( $V_4$ ) are smoothed in parallel.

It is noted that different vertices sets are sequential and the interior of the vertices set is entirely parallel. From the perspective of parallel effects, the above two smooth orderings can

yield the same number of iterations as the sequential algorithm. From the scope of application, the two-color is only applicable to the five-point finite difference format and the four-color can be applied to the nine-point finite difference format. Similarly, the multi-color GS algorithm of the 2D structured grid can be extended to the 3D structured grid.

The popular parallel variant of GS is the red-black GS algorithm based on structured grids and it is not suitable for unstructured grids. As a consequence, the application range of the algorithm is very limited. Moreover, there is also hybrid methods (combining Jacobi and GS), but its convergence rate deteriorates. From the perspective of parallel implementation, the GS algorithm, an essentially sequential algorithm, is not conducive to yield same convergence behavior as the corresponding single-threaded algorithm and obtain high parallel efficiency at the same time.

Finally, we discuss some shortcomings of the standard CPR method.

- (i) Petroleum reservoir simulation is a time-dependent and nonlinear problem. The Jacobian systems need to be solved in each Newton iteration step. The matrix structure of these systems is very similar. The CPR method does not take full advantage of similarity.
- (ii) The CPR method contains many essentially sequential steps in the SETUP, such as which results in low parallel efficiency.
- (iii) The GS method is commonly used as the smoother in the AMG methods. To improve the parallel performance of the smoother, its convergence rate usually deteriorates, and vice versa.

In view of the shortcomings (i) and (ii) mentioned above, we discuss how to reuse similar matrix structures to improve the performance of CPR in Section 4. Furthermore, for the shortcoming (iii), we propose a multi-color GS method from the algebraic point of view in Section 5. We show that the multi-color GS method can not only yield same convergence behavior as the corresponding single-threaded algorithm, but also obtain a good parallel efficiency.

**4. An adaptive SETUP CPR preconditioner.** In this section, we propose an efficient CPR preconditioner using an adaptive SETUP strategy. For the sake of simplicity, we employ CPR as the preconditioner and restarted GMRES as the iterative method (denoted as CPR-GMRES) to illustrate the fundamental idea of the ASCPR preconditioner, and the corresponding algorithm is denoted as ASCPR-GMRES. We develop ASCPR-GMRES to solve efficiently the Jacobian systems and take the right preconditioner as an example to describe its implementation; see Algorithm 4.1 and Algorithm 4.2.

It is noted that the CPR preconditioner  $B^{(k)}$  is generated by exploiting an adaptive strategy in Algorithm 4.1. The concrete implementation of the strategy is as follows; see Algorithm 4.2.

- If  $k = 1$ , the preconditioner  $B^{(1)}$  is generated by calling Algorithm 3.1 (Remark 2);
- If  $k > 1$ , the establishment of the preconditioner  $B^{(k)}$  can be viewed as the following two steps. First of all, we obtain  $It^{(k-1)}$ , which is the number of iterations obtained by solving the previous Jacobian system  $A^{(k-1)}x^{(k-1)} = b^{(k-1)}$ . Furthermore, there are two situations by judging the size of  $It^{(k-1)}$  and  $\mu$  (given a threshold greater than or equal to 0). If  $It^{(k-1)} \leq \mu$ , the preconditioner  $B^{(k)}$  adopts the previous preconditioner  $B^{(k-1)}$ ; otherwise, the preconditioner  $B^{(k)}$  is generated by calling Algorithm 3.1.

**Remark 2.** Algorithm 3.1 is a preconditioning method ( $w = \text{CPR}(A, g, w_0)$  i.e.,  $w = Bg$ ). For the convenience of describing Algorithms 4.1 and 4.2, we assume Algorithm 3.1 creates a CPR preconditioner  $B$ .

**Remark 3.** If the sizes of matrices  $A^{(k-1)}$  and  $A^{(k)}$  are not the same, we must regenerate the preconditioner  $B^{(k)}$ .

We introduce a practical threshold  $\mu$  as a criterion for the adaptive SETUP preconditioner, which aims at improving the performance of the ASCPR-GMRES. To begin with, we explain

**Algorithm 4.1** ASCPR-GMRES method

---

**Input:**  $B^{(k-1)}, It^{(k-1)}, A^{(k)}, b^{(k)}, x_0, \mu, k, m, tol, MaxIt$ ;  
**Output:**  $x^{(k)}, It^{(k)}, B^{(k)}$ ;

- 1  $B^{(k)} = \text{ASCPR}(B^{(k-1)}, It^{(k-1)}, \mu, k)$ ;
- 2 Compute  $r_0 \leftarrow b - A^{(k)}x_0$ ,  $p_1 \leftarrow r_0/\|r_0\|$ ;
- 3 **for**  $It = 1, \dots, MaxIt$  **do**
- 4     **for**  $j = 1, \dots, m$  **do**
- 5         Compute  $\bar{p} \leftarrow A^{(k)}(B^{(k)}p_j)$ ;
- 6         Compute  $h_{i,j} \leftarrow (\bar{p}, p_i), i = 1, \dots, j$ ;
- 7         Compute  $\tilde{p}_{j+1} \leftarrow \bar{p} - \sum_{i=1}^j h_{i,j}p_i$ ;
- 8         Compute  $h_{j+1,j} \leftarrow \|\tilde{p}_{j+1}\|$ ;
- 9         **if**  $h_{j+1,j} = 0$  **then**
- 10              $m \leftarrow j$ ; **break**;
- 11         **end**
- 12         Compute  $p_{j+1} \leftarrow \tilde{p}_{j+1}/h_{j+1,j}$ ;
- 13     **end**
- 14     Solve the following minimization problem:
 
$$y_m = \arg \min_{y \in \mathbb{R}^m} \|\beta e_1 - \bar{H}_m y\|,$$

where  $\beta = \|p_1\|$ ,  $e_1 = (1, 0, \dots, 0)^T \in \mathbb{R}^{m+1}$ ,  $\bar{H}_m := (h_{i,j}) \in \mathbb{R}^{(m+1) \times m}$ ;
- 15      $x_m \leftarrow x_0 + B^{(k)}(P_m y_m)$ , here  $P_m := (p_1, p_2, \dots, p_m)$ ;
- 16     Compute  $r_m \leftarrow b - A^{(k)}x_m$ ;
- 17     **if**  $\|r_m\|/\|r_0\| < tol$  **then**
- 18         **break**;
- 19     **else**
- 20          $x_0 \leftarrow x_m$ ;
- 21          $p_1 \leftarrow r_m/\|r_m\|$ ;
- 22     **end**
- 23 **end**
- 24  $x^{(k)} \leftarrow x_m, It^{(k)} \leftarrow It$ ;
- 25 **return**  $x^{(k)}, It^{(k)}, B^{(k)}$ .

---

the main idea of this approach. The  $It^{(k-1)} \leq \mu$  means  $B^{(k-1)}$  is an effective preconditioner for Jacobian system  $A^{(k-1)}x^{(k-1)} = b^{(k-1)}$  because of the less the number of iterations  $It^{(k-1)}$ , the more  $B^{(k-1)}$  approximates the inverse of matrix  $A^{(k-1)}$ . Because the structure of these matrices is very similar and the CPR preconditioner does not require high accuracy, the preconditioner  $B^{(k-1)}$  can also be used as a preconditioner for Jacobian system  $A^{(k)}x^{(k)} = b^{(k)}$ . Moreover, the approach can improve the performance of the solver from the following two aspects.

- For one thing, the efficiency of the solver is improved because the number of SETUP calls can be reduced.
- For another, the parallel performance of the solver is improved because the proportion of low parallel speedup is reduced in the solver.

Due to choosing a suitable  $\mu$  is very important to the performance of the solver. Finally, we discuss the choice of  $\mu$ . If  $\mu$  is too small, the number of SETUP calls is little reduced. As a result, the performance of the solver has not been significantly improved. Specifically when  $\mu = 0$ , ASCPR-GMRES degenerates into CPR-GMRES. On the contrary, if  $\mu$  is too large, the



**Algorithm 4.2** ASCPR method

---

**Input:**  $B^{(k-1)}, It^{(k-1)}, \mu, k;$   
**Output:**  $B^{(k)};$

- 1 **if**  $k > 1$  *and*  $It^{(k-1)} \leq \mu$  **then**
- 2   |  $B^{(k)} \leftarrow B^{(k-1)};$
- 3 **else**
- 4   | The preconditioner  $B^{(k)}$  is generated by calling Algorithm 3.1.
- 5 **end**
- 6 **return**  $B^{(k)}.$

---

number of iterations of the solver is dramatically increased, thereby affecting the performance of the solver. Generally speaking, the optimal  $\mu$  is determined through numerical experiments according to concrete problems.

**5. A multi-color GS method.** In this section, we propose a parallel GS algorithm from the algebraic point of view, looking forward to overcoming the limitations of the conventional red-black GS algorithm, yielding same convergence behavior as the corresponding single-threaded algorithm and obtaining a good parallel speedup.

To this end, the concept of adjacency graph is introduced. It is noted that an adjacency graph corresponds to a sparse matrix and the nonzero entries of the matrix reflect the connectivity relationship between vertices in the graph. Assume that a sparse matrix  $A \in \mathbb{R}^{n \times n}$  is symmetric. Let  $G_A(V, E)$  be the (undirected) adjacency graph corresponding to the sparse matrix  $A = (a_{ij})_{n \times n}$ , where  $V = \{v_1, v_2, \dots, v_n\}$  is the vertices set and  $E = \{(v_i, v_j) : \forall i \neq j, a_{ij} \neq 0\}$  is the edges set (each nonzero entry  $a_{ij}$  on the non diagonal of  $A$  corresponds to an edge  $(v_i, v_j)$ ).

We are now in the position to give the design goals of this algorithm for grouping vertices and the parallel GS algorithm implementation based on strong connections of  $A$ .

**5.1. Algorithm design goals.** The goal of our algorithm design is to divide the vertices set  $V$  into  $c$  subsets  $V_1, V_2, \dots, V_c$  ( $1 \leq c \leq n$ ) and these subsets shall satisfy the following four conditions:

- (a)  $V = V_1 \cup V_2 \dots \cup V_c;$
- (b)  $V_i \cap V_j = \emptyset, i \neq j, 1 \leq i, j \leq c;$
- (c) Vertices in any subset are not connected, i.e.,  $a_{ij} = a_{ji} = 0, \forall v_i, v_j \in V_\ell (\ell = 1, \dots, c);$
- (d) The number of subsets  $c$  should be as small as possible.

It is easy to see that the smaller the number of groupings  $c$ , the more difficult the grouping and the larger the parallel granularity. The classic GS is, in fact, equivalent to the situation when  $c$  is equal to  $n$ .

**Remark 4.** The red-black GS algorithm also satisfies the above four conditions with  $c = 2$ .

**5.2. Parallel GS algorithm.** In 2003 Saad [12] gave an upper bound estimate of total number of colors based on the graph theory. To proceed, we briefly review this upper bound estimate as follows.

**Proposition 5.1 (Upper bound estimation).** *The number of multi-color groupings  $c$  of undirected graph  $G_A(V, E)$  does not exceed  $\text{degree}(G_A(V, E)) + 1$ , i.e.,  $c$  does not exceed the maximum number of nonzero entries in each row of matrix  $A$ .*

According to Proposition 5.1, the number of groups  $c$  depends on the maximum number of nonzero entries in each row of matrix  $A$ . When the matrix  $A$  is relatively dense (such as the coarse grid matrix in AMG), the number of groups  $c$  is large, which contradicts the condition (d) of Section 5.1. In extreme cases, the row nonzero entries of a matrix can be equal to the



order of the matrix (this implies that  $c = n$ ). Too many groups bring up two difficulties: low efficiency of grouping algorithm and poor parallel performance. For the latter, because there are only small number of degrees of freedom within each group, it results in fine parallel granularity.

For this reason,  $G_A(V, E)$  needs to be preprocessed to strengthen its sparseness before grouping the degrees of freedom. There are many ways to enhance the sparseness of  $G_A(V, E)$ . When the sparseness of  $G_A(V, E)$  is enhanced, the number of groups  $c$  becomes smaller. At the same time, the independence of vertex set  $V_\ell$  ( $\ell = 1, \dots, c$ ) becomes worse, which affects the parallel results. Therefore, choosing an appropriate strategy is of great importance to enhance the sparseness of  $G_A(V, E)$ . The situation is considered where the solution vector is relatively smooth. It is found that the smaller nonzero entries (in the sense of absolute value) in each row of the matrix play a negligible role when a certain degree of freedom is smoothed by GS. In this paper, we propose a strategy to filter small nonzero entries. The matrix, whose small nonzero entries are filtered, is called the so-called “matrix of strong connections”. This concept is defined as follows.

The matrix  $A = (a_{ij})_{n \times n}$  corresponds to the matrix of strong connections  $S(A, \theta)$  (denoted as  $S$ ) and its entries are defined as

$$(5.1) \quad S_{ij} = \begin{cases} 1, & |a_{ij}| > \theta \sum_{k=1}^n |a_{ik}| \\ 0, & |a_{ij}| \leq \theta \sum_{k=1}^n |a_{ik}| \end{cases} \quad \forall i, j = 1, 2, \dots, n, i \neq j,$$

where  $\theta$  ( $0 \leq \theta \leq 1$ ) is a given threshold,  $S_{ij} = 1$  when there is a strong adjacent edge between  $v_i$  and  $v_j$ , and  $S_{ij} = 0$  means that there is no strong adjacent edge between  $v_i$  and  $v_j$ .

To describe our algorithm conveniently, we introduce the following notations.

- The set  $S_i$  represents the vertex set that are strongly connected to the vertex  $v_i$ , i.e.,  $S_i = \{j : S_{ij} \neq 0, j = 1, 2, \dots, n\}$ .
- The set  $\bar{S}_i$  represents the vertex set that are strongly connected to the vertex  $v_i$  (including  $v_i$ ) and whose colors are undetermined. That is,  $\bar{S}_i = \{j : j \in S_i \cup \{i\} \text{ and color of } j \text{ is undetermined}\}$ .
- The set  $\hat{S}_i$  represents the vertex set that are next strongly connected to the vertex  $v_i$  (the vertices on “the second circle”) and whose colors are undetermined. That is,  $\hat{S}_i = \{j : j \in W_i \text{ and color of } j \text{ is undetermined}\}$  where  $W_i = \{j : \forall k \in S_i, j \in S_k / (S_i \cup \{i\})\}$ .
- The cardinality  $|\cdot|$  represents the number of entries in the set  $\cdot$ . In particular,  $|S_i|$  represents the influence value of the vertex  $v_i$ .

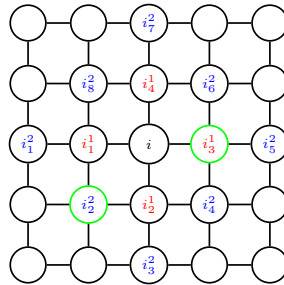


Fig. 3. Schematic diagram of notations explanation.

Let’s explain these notations with a simple schematic diagram, see Fig. 3. Assume that the all edges are strongly adjacent edges in Fig. 3; moreover, the vertices  $i_3^1$  and  $i_2^2$  are given the

splitting attribute (i.e., they have their own color). Hence  $S_i = \{i_1^1, i_2^1, i_3^1, i_4^1\}$ ,  $\bar{S}_i = \{i, i_1^1, i_2^1, i_3^1\}$ ,  $\hat{S}_i = \{i_1^2, i_3^2, i_4^2, i_5^2, i_6^2, i_7^2, i_8^2\}$  and  $|S_i| = 4$ .

In the following, our algorithms are presented. To begin with, we propose a greedy splitting algorithm for the vertices set  $V$  based on the matrix of strong connections (denoted as VerticesSplitting), see Algorithm 5.1. The proposed Algorithm 5.2 gives a vertices grouping algorithm corresponding to the matrix  $A$  (denoted as VerticesGrouping).

---

**Algorithm 5.1** VerticesSplitting method
 

---

**Input:**  $V, S$ ;  
**Output:**  $W, \bar{W}$ ;

- 1 Set  $W \leftarrow \emptyset, \bar{W} \leftarrow \emptyset, \widehat{W} \leftarrow \emptyset$ ;
- 2 **while**  $V \neq \emptyset$  **do**
- 3 **if**  $\widehat{W} \neq \emptyset$  **then**
- 4 | Any take  $v_i \in \widehat{W}$  and  $|S_i| \geq |S_j|, \forall v_i, v_j \in \widehat{W}$ ;
- 5 | **else**
- 6 | Any take  $v_i \in V$  and  $|S_i| \geq |S_j|, \forall v_i, v_j \in V$ ;
- 7 | **end**
- 8 **if**  $v_i$  is not strongly connected to any vertices in the set  $W$  (i.e.,  $S_{ij} = 0, \forall j \in W$ ) **then**
- 9 |  $W \leftarrow W \cup v_i, V \leftarrow V/v_i$ ;
- 10 | **if**  $v_i \in \widehat{W}$  **then**
- 11 | |  $\widehat{W} \leftarrow \widehat{W}/v_i$ ;
- 12 | | **end**
- 13 |  $\bar{W} \leftarrow \bar{W} \cup S_i$ ;
- 14 |  $V \leftarrow V/S_i$ ;
- 15 |  $\widehat{W} \leftarrow \widehat{W} \cup \hat{S}_i$ ;
- 16 | **else**
- 17 |  $\bar{W} \leftarrow \bar{W} \cup v_i$ ;
- 18 |  $V \leftarrow V/v_i$ ;
- 19 | **if**  $v_i \in \widehat{W}$  **then**
- 20 | |  $\widehat{W} \leftarrow \widehat{W}/v_i$ ;
- 21 | | **end**
- 22 | **end**
- 23 **end**
- 24 **return**  $W, \bar{W}$ .

---



---

**Algorithm 5.2** VerticesGrouping method
 

---

**Input:**  $V, S$ ;  
**Output:**  $V_\ell$  ( $\ell = 1, \dots, c$ );

- 1 Set  $c \leftarrow 0$ ;
- 2 **while**  $V \neq \emptyset$  **do**
- 3 |  $c \leftarrow c + 1$ ;
- 4 | Call Algorithm 5.1 to generate  $V_c$  and  $\bar{V}_c$ ;
- 5 | Let  $V \leftarrow \bar{V}_c$ ;
- 6 **end**
- 7 **return**  $V_\ell$  ( $\ell = 1, \dots, c$ ).

---

As can be easily noticed from Algorithms 5.1 and 5.2, the grouping numbers  $c$  and the degree of independence of vertices set  $V_\ell$  ( $\ell = 1, \dots, c$ ) depend on the choice of strength threshold  $\theta$ .

The smaller the value of  $\theta$ , the better the degree of independence of vertices set, but the greater the  $c$ . Especially when  $\theta = 0$ , the degree of independence of vertices set is the best (complete independence) but  $c$  is the largest. Moreover, when  $\theta = 1$ , the degree of independence of vertices set is the worst and  $c = 1$  (at this time, the proposed algorithm degenerates to the classic GS algorithm). In this sense, it is necessary to balance the grouping numbers and the degree of independence within the vertices set. In order to better satisfy condition (d), we use an approach to weaken the condition (c) slightly in our algorithms. We expect that this approach can slightly improve the parallel performance.

Next, two properties of our proposed algorithms are given.

**Proposition 5.2 (Matrix diagonalization).** *The block matrix  $A_{V_\ell V_\ell}$  (with  $V_\ell$  as the row and column indices,  $\ell = 1, \dots, c$ ) is the diagonal matrix if the row and column indices of matrix  $A$  are rearranged by the indices set  $\{V_\ell\}_{\ell=1}^c$ .*

**Proposition 5.3 (Finite termination).** *Algorithm 5.2 terminates within a finite number of steps, i.e.,  $c \leq |V|$ .*

*Proof.* To prove that Algorithm 5.2 terminates within a finite step, just prove  $V_c \neq \emptyset$  in line 4 of Algorithm 5.2. According to Algorithm 5.1, if  $V \neq \emptyset$ ,  $V_c$  (i.e., the output variable  $W$  of Algorithm 5.1) contains at least one vertex. From the 2-6 lines of Algorithm 5.2,  $c \leq |V|$  can be obtained. ■

It is noted that the Algorithm 5.2 can split  $G_A(V, E)$  into subgraphs  $G_{A_\ell}(V_\ell, E_\ell)$ ,  $\ell = 1, \dots, c$ . The  $S(A_\ell, \theta)$  is denoted as the adjacency matrix corresponding to each subgraph. And each subgraph corresponds to a submatrix  $A_\ell(V_\ell)$  of matrix  $A$ . According to Proposition 5.2, the diagonal blocks of the submatrix  $A_\ell(V_\ell)$  are diagonal, the GS smoothing of the submatrix  $A_\ell(V_\ell)$  is completely parallel at this time. Furthermore, a parallel (or multi-color) GS algorithm based on the strong connections of matrix is given by Algorithm 5.3, denoted as PGS-SCM.

---

#### Algorithm 5.3 PGS-SCM method

---

**Input:**  $A, x, b, \theta$ ;

**Output:**  $x$ ;

- 1 Using the matrix  $A$  and the formula (5.1) to generate vertices set  $V$  and matrix of strong connections  $S$ , respectively;
  - 2 Call Algorithm 5.2 to generate independent vertices subset  $V_\ell$  ( $\ell = 1, \dots, c$ );
  - 3 Using  $V_\ell$  to split the matrix  $A$  into submatrix  $A_\ell$  ( $\ell = 1, \dots, c$ );
  - 4 **for**  $\ell = 1, \dots, c$  **do**
  - 5 | Parallel call the classic GS algorithm of submatrix  $A_\ell$ ;
  - 6 **end**
  - 7 **return**  $x$ .
- 

Finally, the proposed algorithms can be parallelized for multi-core and many-core architectures. We develop the OpenMP version and the CUDA version of the parallel program, respectively. Furthermore, these algorithms are integrated into the FASP framework (see [46] for more details). The results of the numerical experiments will be given in the next section.

**6. Numerical experiments.** In this section, a three-phase benchmark problem is obtained by changing the fluid properties of the original two-phase SPE10 [49]. Its model dimensions are  $1200 \times 2200 \times 170$  (ft) and the number of grid cells is  $60 \times 220 \times 80$  (the total number of grid cells is 1,122,000 and the number of active cells is 1,094,422). Firstly, we verify convergence behavior and parallel performance for the PGS-SCM method. Furthermore, we test the correctness and parallel performance for the ASCPR-GMRES-OMP and ASCPR-GMRES-CUDA methods,

where the ASCPR-GMRES-OMP and ASCPR-GMRES-CUDA correspond to OpenMP version and CUDA version solvers, respectively.

We now introduce some details of the ASCPR-GMRES method. For the CPR preconditioner, in the first stage, we use the Unsmoothed Aggregation AMG (UA-AMG) method [21,50] to approximate the inverse of the pressure coefficient matrix, where the aggregation strategy is the so-called non-symmetric pairwise matching aggregation (NPAIR) [51], the cycle type is the Nonlinear AMLI-cycle [52,53], the smoothing operator is PGS-SCM, the degree of freedom of the coarsest space is 10000, and the coarsest space solver is the PARDISO [54] direct method. And in the second stage, we use the BILU method based on Level Scheduling (LS) [12] to approximate the inverse of the whole coefficient matrix. For the GMRES method, the number of restart  $m$  is 28, the maximum number of iterations  $MaxIt$  is 100 and the tolerance error of relative residual norm  $tol$  is  $10^{-5}$ .

Finally, the numerical examples are tested on a machine with Intel Xeon Platinum 8260 CPU (32 cores, 2.40GHz), 128GB RAM and NVIDIA Tesla T4 GPU (16GB Memory).

**6.1. PGS-SCM method.** To explore the convergence behavior and parallel performance of the proposed PGS-SCM method, we employ the CPR-GMRES method as the solver for petroleum reservoir simulation. Furthermore, we employ the parallel GS method based on natural ordering (denoted as PGS-NO) as a reference for comparison.

**Example 6.1.** The three-phase example is considered and the numerical simulation time is conducted for 100 days. We use the different number of threads ( $NT = 1, 2, 4, 8, 16$ ) to test parallel performance of CPR-GMRES-PGS-NO and CPR-GMRES-PGS-SCM. The impacts of the different strength thresholds  $\theta$  ( $\theta = 0, 0.05, 0.1, 0.3$ ) on CPR-GMRES-PGS-SCM are also tested.

Tab. 1 lists the experimental results of Example 6.1, such as the total number of linear iterations ( $Iter$ ), the total solution time ( $Time$ ) and the parallel speedup ( $Speedup$ , see Remark 5 for the calculation formula).

**Tab. 1**  
*Iter, Time(s) and Speedup of the two solvers with different NT.*

Solvers	$\theta$	NT	1	2	4	8	16
CPR-GMRES-PGS-NO	—	<i>Iter</i>	3336	3338	3372	3439	3527
		<i>Time</i>	3406.71	2050.70	1258.79	804.38	687.76
		<i>Speedup</i>	1.00	1.66	2.71	4.24	4.95
CPR-GMRES-PGS-SCM	0	<i>Iter</i>	<b>3334</b>	<b>3334</b>	<b>3334</b>	<b>3334</b>	<b>3334</b>
		<i>Time</i>	3489.93	1937.48	1125.65	723.21	608.78
		<i>Speedup</i>	1.00	1.80	3.10	4.83	<b>5.73</b>
	0.05	<i>Iter</i>	3236	3236	3237	3237	<b>3237</b>
		<i>Time</i>	3446.89	1920.54	1102.48	711.16	<b>598.86</b>
		<i>Speedup</i>	1.00	1.79	3.13	4.85	<b>5.76</b>
	0.1	<i>Iter</i>	3379	3381	3381	3385	3385
		<i>Time</i>	3551.89	1976.98	1141.65	745.85	624.98
		<i>Speedup</i>	1.00	1.80	3.11	4.76	5.68
	0.3	<i>Iter</i>	3314	3315	3470	3496	3477
		<i>Time</i>	3421.46	1909.81	1154.44	756.08	631.75
		<i>Speedup</i>	1.00	1.79	2.96	4.53	5.42

**Remark 5.** The calculation formula of Speedup is

$$Speedup = \frac{T_1}{T_n}$$

where  $T_1$  represents the wall time obtained by a single thread (core) and  $T_n$  represents the wall time obtained by  $n$  threads (cores).

It can be seen from Tab.1 that, for CPR-GMRES-PGS-NO solver, the total number of linear iterations is gradually increasing as NT increases. When NT = 16, the total number of linear iterations is increased by 191 compared with the single-threaded result and the speedup is 4.95. This implies that the number of iterations of the parallel GS algorithm based on natural ordering is not stable. That is, as the number of threads increases, the number of iterations increases, which affects parallel speedup of the solver. On the other hand, for CPR-GMRES-PGS-SCM solver (when  $\theta = 0$ ), the total number of linear iterations is not changed with larger NT. Such results indicate that the proposed PGS-SCM yields same convergence behavior as the corresponding single-threaded algorithm, which verifies the effectiveness of the algorithm. Moreover, from the perspective of parallel performance, CPR-GMRES-PGS-SCM gets a higher speedup compared with CPR-GMRES-PGS-NO. For example, when NT = 16, the speedup of CPR-GMRES-PGS-SCM increases to 5.73 (from 4.95 to 5.73). Hence, the proposed PGS-SCM method can obtain a better parallel speedup.

Next, we discuss the influence of different strength thresholds  $\theta$  on the parallel performance for CPR-GMRES-PGS-SCM solver. When  $\theta$  is small (for example,  $\theta = 0, 0.05$ ), the total number of linear iterations is changed very little with the increase of NT and can even be considered unchanged. But when  $\theta$  is larger (for example,  $\theta = 0.1, 0.3$ ), the varied range of the total number of linear iterations is enlarged with the increase of NT. These results show that as  $\theta$  increases, the independence of the degrees of freedom is decreased; thus, which affects the number of iterations. If NT = 16 is considered, the proposed method obtains some meaningful results. As  $\theta$  increases, the total number of linear iterations firstly is decreased and then is increased, and the speedup firstly is increased and then is decreased. Especially when  $\theta = 0.05$ , the minimum total number of linear iterations is 3237 and the speedup is the highest, reaching 5.76. All in all, the strength threshold  $\theta$  affects the stability of the number of iterations and parallel performance. In this experiment, when  $\theta = 0.05$ , the obtained number of iterations is the least and the parallel speedup is the highest.

**6.2. ASCPR-GMRES-OMP method.** In order to verify the correctness and parallel performance of ASCPR-GMRES-OMP, we discuss the influences of different thresholds  $\mu$  on the experimental results.

**Example 6.2.** For the three-phase example, the numerical simulation is conducted for 100 days and  $\theta = 0.05$ . We explore the parallel performance of ASCPR-GMRES-OMP for five groups of  $\mu$  (i.e.,  $\mu = 0, 10, 20, 30, 40$ ), when NT = 1, 2, 4, 8, 16, respectively.

First of all, to verify the correctness of ASCPR-GMRES-OMP, we present respectively the field oil production rate and average pressure graphs of five groups  $\mu$  (when NT = 16), see Fig. 4(a) and Fig. 4(b).

From the Fig. 4(a) and Fig. 4(b), we can see that the field oil production rate and average pressure obtained by the adaptive SETUP CPR preconditioner ( $\mu = 10, 20, 30, 40$ ) and the general CPR preconditioner ( $\mu = 0$ ) completely coincide, indicating that ASCPR-GMRES-OMP method is correct.

In order to fairly compare the parallel speedup of ASCPR-GMRES-OMP, we propose a

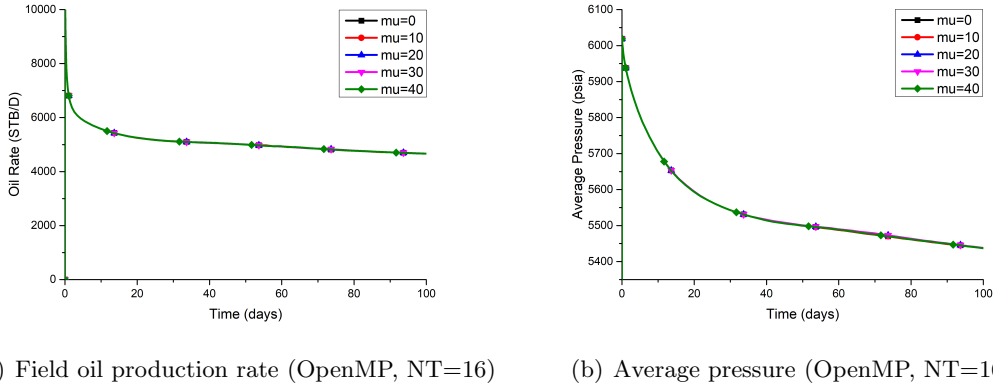


Fig. 4. Comparison charts of field oil production rate and average pressure of five groups  $\mu$ .

new parallel speedup (denoted as  $Speedup^*$ ) and its calculation formula is as follows:

$$Speedup^* = \frac{T_1^0}{T_n^\mu}$$

where  $T_1^0$  represents the wall time obtained by a single thread (core) when the general preconditioner ( $\mu = 0$ ) are used and  $T_n^\mu$  represents the wall time obtained by  $n$  threads (cores) when the adaptive SETUP preconditioner threshold is  $\mu$ .

Then, we also discuss the impacts of different thresholds  $\mu$  on the parallel speedup of ASCPR-GMRES-OMP. Tab. 2 lists the number of SETUP calls ( $SetupCalls$ ), the ratio of SETUP in the total solution time ( $SetupRatio$ ), the total number of linear iterations ( $Iter$ ), total solution time ( $Time$ ), new parallel speedup ( $Speedup^*$ ) and parallel speedup ( $Speedup$ ).

According to the results of Tab. 2, we firstly discuss the number of SETUP calls, the ratio of SETUP in the total solution time and the total number of linear iterations. For the number of SETUP calls and the ratio of SETUP in the total solution time, when NT is fixed, both the number of SETUP calls and the ratio of SETUP in the total solution time are decreasing as  $\mu$  increases. Especially when  $\mu = 40$ , the number of SETUP calls only takes 13 times. When  $\mu$  is fixed, the number of SETUP calls is not changed with the increase of NT, but the ratio of SETUP in the total solution time is gradually increased (this also reflects fact that the parallel speedup of SOLVE is higher than the parallel speedup of SETUP). For the total number of linear iterations, when NT is fixed, the total number of linear iterations is gradually increasing as  $\mu$  increases. In short, these results indicate that the number of SETUP calls is significantly decreased with the increase of  $\mu$ , but the total number of linear iterations is also increased.

What's more, we discuss the the total solution time and the new parallel speedup (only discuss the impacts of the change of  $\mu$  on the results). Let's take NT=16 as an example. When  $\mu$  increases by 0,10,20,30,40 in turn, the total solution time firstly is decreased and then is increased, and the new parallel speedup firstly is increased and then is decreased. Especially when  $\mu = 20$ , the total solution time is 522.75 (s) and the corresponding the new parallel speedup is 6.59. Compared with the case of the general CPR preconditioner, the total solution time of ASCPR-GMRES-OMP is reduced from 598.86 (s) to 522.75 (s) and the the new parallel speedup is increased from 5.76 to 6.59. These show that the proposed method can further improve the parallel performance of the solver.

Finally, we still discuss the changes in the parallel speedup. As  $\mu$  increases, the parallel speedup is increased. Specially when  $\mu = 40$  and NT = 16, the parallel speedup reaches 7.26.

**Tab. 2**  
*SetupCalls, SetupRatio, Iter, Time(s), Speedup\* and Speedup of different  $\mu$  and NT.*

	$\mu$	1	2	4	8	16
<i>SetupCalls</i>	0	178	178	178	178	178
	10	141	141	141	141	141
	20	98	98	98	98	98
	30	25	25	25	25	25
	40	13	13	13	13	13
<i>SetupRatio</i>	0	13.13%	16.51%	22.06%	30.68%	40.44%
	10	12.04%	15.01%	19.88%	28.25%	38.75%
	20	8.76%	10.73%	14.05%	20.74%	33.23%
	30	5.33%	6.23%	8.11%	11.39%	25.06%
	40	4.67%	5.47%	6.91%	10.53%	19.83%
<i>Iter</i>	0	3236	3236	3237	3237	3237
	10	3253	3253	3253	3253	3253
	20	3464	3463	3460	3461	3460
	30	3891	3891	3890	3889	3996
	40	4111	4111	4118	4125	4106
<i>Time</i>	0	3446.89	1920.54	1102.48	711.16	598.86
	10	3348.65	1853.37	1080.48	685.87	573.68
	<b>20</b>	<b>3446.32</b>	<b>1885.40</b>	<b>1063.75</b>	<b>654.28</b>	<b>522.75</b>
	30	3973.86	2145.97	1165.28	676.72	558.70
	40	4229.11	2239.03	1210.80	717.30	582.31
<i>Speedup*</i>	0	1.00	1.79	3.13	4.85	5.76
	10	1.03	1.86	3.19	5.03	6.01
	<b>20</b>	<b>1.00</b>	<b>1.83</b>	<b>3.24</b>	<b>5.27</b>	<b>6.59</b>
	30	0.87	1.61	2.96	5.09	6.17
	40	0.82	1.54	2.85	4.81	5.92
<i>Speedup</i>	0	1.00	1.79	3.13	4.85	5.76
	10	1.00	1.81	3.10	4.88	5.84
	20	1.00	1.83	3.24	5.27	6.59
	30	1.00	1.85	3.41	5.87	7.11
	40	1.00	1.89	3.49	5.90	7.26

These results are consistent with what we expected. However, our goal is not to pursue the highest parallel speedup but to pursue the highest new parallel speedup (or the shortest total solution time).

**6.3. ASCPR-GMRES-CUDA method.** In order to verify the correctness and parallel performance of ASCPR-GMRES-CUDA, we explore the influences of different thresholds  $\mu$  on the experimental results.

**Example 6.3.** For the three-phase example, the numerical simulation is conducted for 100 days and  $\theta = 0.05$ . We explore the impacts of  $\mu$  ( $\mu = 0, 10, 20, 30, 40$ ) on the parallel performance of ASCPR-GMRES-CUDA.

To begin with, to verify the correctness of ASCPR-GMRES-CUDA, we display the field oil production rate and average pressure graphs of five sets  $\mu$ , as shown in Fig. 5(a) and Fig. 5(b), respectively.

From Fig. 5(a) and Fig. 5(b), we can see that the field oil production rate and average pressure obtained by the adaptive SETUP CPR preconditioner (i.e.,  $\mu = 10, 20, 30, 40$ ) and



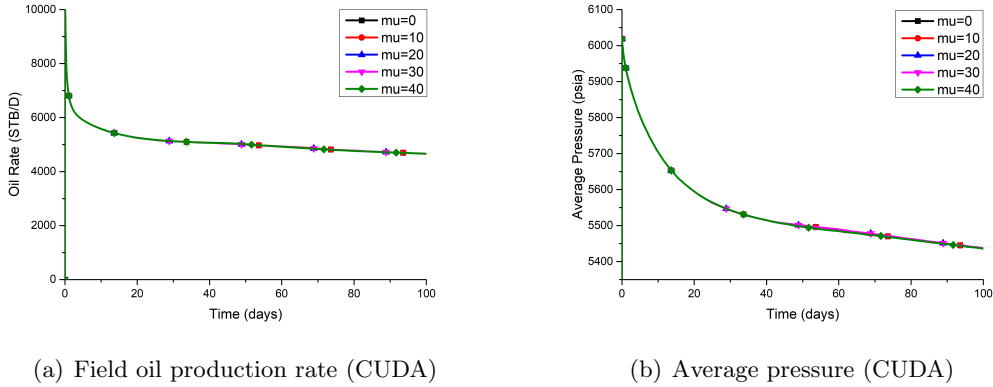


Fig. 5. The field oil production rate and average pressure comparison chart of five sets  $\mu$ .

the general CPR preconditioner (i.e.,  $\mu = 0$ ) completely coincide, indicating that the ASCPR-GMRES-CUDA is correct.

In addition, we study the parallel performance of the ASCPR-GMRES-CUDA. Tab. 3 lists *SetupCalls*, *SetupRatio*, *Iter*, *Time* and *Speedup* of ASCPR-GMRES-CUDA. The single-threaded calculation results of the OpenMP version program (denoted as ASCPR-GMRES-OMP(1)) are also added for comparison.

Tab. 3  
*SetupCalls*, *SetupRatio*, *Iter*, *Time(s)* and *Speedup* of the different  $\mu$ .

Solvers	$\mu$	<i>SetupCalls</i>	<i>SetupRatio</i>	<i>Iter</i>	<i>Time</i>	<i>Speedup</i>
ASCPR-GMRES-OMP(1)	0	178	13.13%	3236	3446.89	—
ASCPR-GMRES-CUDA	0	178	74.01%	3270	594.96	5.79
	10	146	70.97%	3302	534.33	6.45
	20	69	61.20%	3424	413.12	8.34
	<b>30</b>	<b>24</b>	<b>46.24%</b>	<b>4065</b>	<b>355.80</b>	<b>9.69</b>
	40	17	44.21%	4239	362.97	9.50

It can be seen from Tab. 3 that, for ASCPR-GMRES-CUDA solver, as  $\mu$  increases, both the number of SETUP calls and the ratio of SETUP in the total solution time are decreased, the total number of linear iterations is gradually increased and the parallel speedup firstly is increased and then is decreased. The CUDA version can be 5.79 times faster than the ASCPR-GMRES-OMP(1) (when  $\mu = 0$ ). Especially when  $\mu = 30$ , compared with  $\mu = 0$ , the total solution time of ASCPR-GMRES-CUDA is reduced from 594.96 (s) to 355.80 (s), which can be 1.67 times faster. At the same time, compared with ASCPR-GMRES-OMP(1), the speedup of ASCPR-GMRES-CUDA reaches 9.69. Therefore, the proposed method obtains distinct acceleration effects and is more suitable for GPU architecture.

**7. Conclusions.** In this paper, we investigated an efficient parallel CPR preconditioner for the linear algebraic systems arising from the fully implicit discretization of the black oil model. First of all, for two difficulties of the preconditioner, the computation cost is large and the parallel speedup is low in SETUP. We proposed an adaptive SETUP CPR preconditioner to improve the efficiency and parallel performance of the preconditioner. Furthermore, we proposed an efficient parallel GS algorithm based on the coefficient matrix of strong connections. The algorithm can be adapted to unstructured grids, yielded same convergence behavior as the corresponding single-threaded algorithm and obtained a good parallel speedup. In the future, parallel performance of the adaptive SETUP multi-stage preconditioners needs to be further

improved. This paper only considers OpenMP and CUDA implementations for the proposed parallel GS algorithm and further research will be conducted for MPI parallelism.

**Acknowledgments.** This work was supported by the Postgraduate Scientific Research Innovation Project of Hunan Province grants CX20210607 and XDCX2021B110. Feng was partially supported by the Excellent Youth Foundation of SINOPEC(P20009). Zhang was partially supported by the National Science Foundation of China grant 11971472. Shu was partially supported by the National Science Foundation of China grant 11971414. The authors would like to thank the members of the research group of Xiangtan University for their valuable opinions. The authors also appreciate various valuable comments from an anonymous referee on the early version of this paper.

## REFERENCES

- [1] D.W. Peaceman. Fundamentals of numerical reservoir simulation. *Developments in Petroleum Science*, 1977.
- [2] K. Aziz and A. Settari. Petroleum reservoir simulation. *Applied Science Publishers*, 1979.
- [3] Z.X. Chen, G.R. Huan, and Y.L. Ma. Computational methods for multiphase flows in porous media. *Society for Industrial and Applied Mathematics*, 2006.
- [4] J.W. Sheldon, B. Zondek, and W.T. Cardwell. One-dimensional, incompressible, noncapillary, two-phase fluid flow in a porous medium. *Transactions of the AIME*, 207(1):136–143, 1959.
- [5] J. Douglas, Jr., D.W. Peaceman, and H.H. Rachford, Jr. A method for calculating multi-dimensional immiscible displacement. *Transactions of the AIME*, 216:297–308, 1959.
- [6] H.L. Stone and A.O. Garder, Jr. Analysis of gas-cap or dissolved-gas drive reservoirs. *Society of Petroleum Engineers Journal*, 1:92–104, 1961.
- [7] D.A. Collins, L.X. Nghiem, Y.K. Li, and J.E. Grabonstotter. An efficient approach to adaptive-implicit compositional simulation with an equation of state. *SPE Reservoir Engineering*, 7(02):259–264, 1992.
- [8] ECLIPSE. <https://www.software.slb.com/products/eclipse>.
- [9] CMG IMEX. <https://www.cmgl.ca/imex>.
- [10] SENSOR: System for efficient numerical simulation of oil recovery. <https://www.coatsengineering.com/>.
- [11] T.A. Davis. Direct methods for sparse linear systems. *Society for Industrial and Applied Mathematics*, 2006.
- [12] Y. Saad. Iterative methods for sparse linear systems. *Society for Industrial and Applied Mathematics*, 2003.
- [13] J.T. Camargo, J.A. White, N. Castelletto, and R.I. Borja. Preconditioners for multiphase poromechanics with strong capillarity. *International Journal for Numerical and Analytical Methods in Geomechanics*, 45(9).
- [14] J.C. Xu. Iterative methods by space decomposition and subspace correction. *SIAM Review*, 34(4):581–613, 1992.
- [15] J.C. Xu. The auxiliary space method and optimal multigrid preconditioning techniques for unstructured grids. *Computing*, 56(3):215–235, 1996.
- [16] J.A. Meyerink. Iterative methods for the solution of linear equations based on incomplete block factorization of the matrix. *SPE Reservoir Simulation Conference*, SPE-12262, 1983.
- [17] P. Concus, G. H. Golub, and G. Meurant. Block preconditioning for the conjugate gradient method. *SIAM Journal on Scientific and Statistical Computing*, 6(1):220–252, 1985.
- [18] A. Brandt, S.F. McCormick, and J.W. Ruge. Algebraic multigrid (AMG) for sparse matrix equations. In *Sparsity and its Applications*. Cambridge University Press, 1984.
- [19] R.D. Falgout. An introduction to algebraic multigrid computing. *Computing in Science and Engineering*, 8(6):24–33, 2006.
- [20] J.W. Ruge and K. Stüben. Efficient solution of finite difference and finite element equations. *Multigrid Methods for Integral & Differential Equations*, pages 169–212, 1985.
- [21] V.E. Bulgakov. Multi-level iterative technique and aggregation concept with semi-analytical preconditioning for solving boundary-value problems. *Communications in Numerical Methods in Engineering*, 9(8):649–657, 1993.
- [22] Y. Notay. An aggregation-based algebraic multigrid method. *Electronic Transactions on Numerical Analysis Etna*, 37, 2010.
- [23] J.J. Brannick and R.D. Falgout. Compatible relaxation and coarsening in algebraic multigrid. *SIAM Journal on Scientific Computing*, 32(3):1393–1416, 2010.
- [24] H.D. Sterck, U.M. Yang, and J.H. Jeffrey. Reducing complexity in parallel algebraic multigrid preconditioning.

- tioners. *SIAM Journal on Matrix Analysis and Applications*, 27(4):1019–1039, 2006.
- [25] A. Napov and Y. Notay. An algebraic multigrid method with guaranteed convergence rate. *SIAM Journal on Scientific Computing*, 34(2):A1079–A1109, 2012.
- [26] J.R. Wallis. Incomplete gaussian elimination as a preconditioning for generalized conjugate gradient acceleration. *SPE Reservoir Simulation Conference*, SPE-12265, 1983.
- [27] J.R. Wallis, R.P. Kendall, and T.E. Little. Constrained residual acceleration of conjugate residual methods. *SPE Reservoir Simulation Conference*, SPE-13536, 1985.
- [28] H. Cao, H.A. Tchelepi, J.R. Wallis, and H.E. Yardumian. Parallel scalable unstructured CPR-Type linear solver for reservoir simulation. *SPE Annual Technical Conference and Exhibition*, SPE-96809, 2005.
- [29] Z. Li, S.H. Wu, C.S. Zhang, J.C. Xu, C.S. Feng, and X.Z. Hu. Numerical studies of a class of linear solvers for fine-scale petroleum reservoir simulation. *Computing & Visualization in Science*, 18(2-3):93–102, 2017.
- [30] K. Stüben, T. Clees, H. Klie, B. Lu, and M.F. Wheeler. Algebraic multigrid methods (AMG) for the efficient solution of fully implicit formulations in reservoir simulation. *SPE Reservoir Simulation Conference*, SPE-105832, 2007.
- [31] T.M. Al-Shaalan, H.M. Klie, A.H. Dogru, and M.F. Wheeler. Studies of robust two stage preconditioners for the solution of fully implicit multiphase flow problems. *SPE Reservoir Simulation Conference*, SPE-118722, 2009.
- [32] X.Z. Hu, J.C. Xu, and C.S. Zhang. Application of auxiliary space preconditioning in field-scale reservoir simulation. *SCIENCE CHINA Mathematics*, 56(12):2737–2751, 2013.
- [33] A.H. Dogru, L.S.K. Fung, U. Middy, T. Al-Shaalan, and J.A. Pita. A next-generation parallel reservoir simulator for giant reservoirs. SPE-119272, 2009.
- [34] E.M. Hayder and M. Baddourah. Challenges in high performance computing for reservoir simulation. All Days, 06 2012.
- [35] C.S. Feng, S. Shu, J.C. Xu, and C.S. Zhang. A multi-stage preconditioner for the black oil model and its OpenMP implementation. *Lecture Notes in Computational Science and Engineering*, 98:141–153, 2014.
- [36] S.H. Wu, J.C. Xu, C.S. Feng, C.S. Zhang, Q.Y. Li, S. Shu, B.H. Wang, X.B. Li, and H. Li. A multi-level preconditioner and its shared memory implementation for a new generation reservoir simulator. *Petroleum Science*, 2014.
- [37] M. Mesbah, A. Vatani, M. Siavashi, and M.H. Doranehgard. Parallel processing of numerical simulation of two-phase flow in fractured reservoirs considering the effect of natural flow barriers using the streamline simulation method. *International Journal of Heat and Mass Transfer*, 131:574–583, 2019.
- [38] H.J. Yang, S.Y. Sun, Y.T. Li, and C. Yang. Parallel reservoir simulators for fully implicit complementarity formulation of multicomponent compressible flows. *Computer Physics Communications*, 244:2–12, 2019.
- [39] S.H. Wu, B.H. Wang, Q.Y. Li, J.C. Xu, C.S. Zhang, and C.S. Feng. Cost-effective parallel reservoir simulation on shared memory. *SPE Asia Pacific Oil and Gas Conference and Exhibition*, All Days, 2016.
- [40] L.F. Werneck, M.M. de Freitas, G. de Souza, L.F.C. Jatobá, and H.P. Amaral Souto. An OpenMP parallel implementation using a coprocessor for numerical simulation of oil reservoirs. *Computational and Applied Mathematics*, 38, 2019.
- [41] B.H. Wang, S.H. Wu, Q.Y. Li, X.B. Li, H. Li, C.S. Zhang, and J.C. Xu. A multilevel preconditioner and its shared memory implementation for new generation reservoir simulator. *SPE Large Scale Computing and Big Data Challenges in Reservoir Simulation Conference and Exhibition*, SPE-172988, 2014.
- [42] H. Sudan, H. Klie, R. Li, and Y. Saad. High performance manycore solvers for reservoir simulation. *European Conference on the Mathematics of Oil Recovery*, 2010.
- [43] Z.J. Kang, Z. Deng, W. Han, and D.M. Zhang. Parallel reservoir simulation with OpenACC and domain decomposition. *Algorithms*, 11(12), 2018.
- [44] B. Yang, H. Liu, and Z.X. Chen. Accelerating linear solvers for reservoir simulation on GPU workstations. *Society for Computer Simulation International*, 2016.
- [45] P. Lian, B. Ji, T. Duan, H. Zhao, and X. Shang. Parallel numerical simulation for a super large-scale compositional reservoir. *Advances in Geo-Energy Research*, 4(3):381–386, 2019.
- [46] FASP: Fast auxiliary space preconditioning. <http://www.multigrid.org/fasp/>.
- [47] METIS: Serial graph partitioning and fill-reducing matrix ordering. <http://glaros.dtc.umn.edu/gkhome/metis/metis/overview>.
- [48] J.A. Trangenstein and J.B. Bell. Mathematical structure of the black-oil model for petroleum reservoir simulation. *SIAM Journal on Applied Mathematics*, 49(3):749–783, 1989.
- [49] M.A. Christie and M.J. Blunt. Tenth SPE comparative solution project: A comparison of upscaling techniques. *SPE Reservoir Evaluation & Engineering*, 4(04):308–317, 2001.
- [50] D. Braess. Towards algebraic multigrid for elliptic problems of second order. *Computing*, 55(4):379–393, 1995.

- 
- [51] A. Napov and Y. Notay. An algebraic multigrid method with guaranteed convergence rate. *SIAM Journal on Scientific Computing*, 34(2):A1079–A1109, 2012.
  - [52] J.K. Kraus. An algebraic preconditioning method for M-matrices: linear versus non-linear multilevel iteration. *Numerical Linear Algebra with Applications*, 2002.
  - [53] X.Z. Hu, P.S. Vassilevski, and J.C. Xu. Comparative convergence analysis of nonlinear AMLI-Cycle multigrid. *SIAM Journal on Numerical Analysis*, 51(2):1349–1369, 2013.
  - [54] PARDISO: Parallel direct sparse solver interface. <https://www.pardiso-project.org>.